Grant Agreement No: 101096307

Full Title: THz Industrial Mesh Networks in Smart Sensing and Propagation Environments

Start date: 01/01/2023

End date: 31/03/2026

Duration: 39 Months

Deliverable D2.4

Updated report on scenario and KPI coherence

Document Type	Deliverable
Title	D2.4 Updated report on scenario and KPI coherence
Contractual due date	31/03/2026 (M39)
Actual submission date	31/03/2026
Nature	Report
Dissemination Level	PUB
Lead Beneficiary	AETNA
Responsible Author	Gabriele Canini (AETNA)
Contributions from	Gabriele Canini (AETNA), Carlo Lanzoni (AETNA), Francesco Meoni (BI-REX), Tommaso Zugno (HWDU), Thomas Kurner (TUBS), Sebastien Chartier (FRAUNHOFER), Guillaume Ducournau (CNRS), Victor Torres (ANT)
Reviewers	Victor Torres (ANT), Giacomo Bacci (CNIT)

6GSNS

Revision history

Version	Issue Date	Changes	Contributor(s)
V0.0	21/02/2026	Emission	Gabriele Canini (AETNA)
V0.1	08/03/2026	Chapter 2.1 Critical Comment on USE CASES and KPI	Gabriele Canini (AETNA), Francesco Meoni (BI-REX), Varvara Elesina (TUBS), Carlo Lanzoni (AETNA)
V0.2	16/03/2026	Critical Comment to D2.2 - Definition of scenarios for software simulation	Tommaso Zugno (HWDU)
V0.3	27/03/2026	• Integration in Chapter 2.1 Critical Comment on USE CASES and KPI • Critical Comment to D2.3 - Definition of the scenarios and KPI for HW demonstration and PoC	Thomas Kurner (TUBS), Sebastien Chartier (FRAUNHOFER), Guillaume Ducournau (CNRS) Victor Torres (ANT)
V0.4	28/03/2026	Global review	Gabriele Canini(AETNA)
V0.5	31/03/2026	Final Review	Victor Torres (ANT), Giacomo Bacci (CNIT)
V1.0	05/04/2026	Final version approved	Luca Sanguinetti (CNIT), Thomas Kurner (TUBS)

Table of contents

List of Abbreviations

6G	6th Generation
AGV	Automated Guided Vehicle
AMR	Autonomous Mobile Robot
AR	Augmented Reality
AR	Augmented Reality
ARQ	Automatic Repeat Request
AS	Azimuth Spread
B5G	Beyond 5G
CIR	Complex Impulse Response
CNC	Computer Numerical Control
DS	Delay Spread
EMF	Electromagnetic Field
ES	Elevation Spread
FSO	Free-Space Optics
HMI	Human Machine Interface
HMI	Human Machine Interface
HTTP	Hyper-Text Transfer Protocol
IRS	Intelligent Reflecting Surfaces
ISAC	Integrated Sensing and Communications
KPI	Key Performance Indicator
KPI	Key Performance Indicator
LGV	Laser Guided Vehicle
LIDAR	LIght Detection And Ranging
MAC	Medium Access
MIMO	Multiple Input – Multiple Output
MTP	Motion-to-Photon
NLOS	Non-Line-of-Sight
OEE	Overall Equipment Effectiveness
OPC/UA	Open Platform Communications Unified Architecture
PAP	Power Azimuth Profile
PDP	Power Delay Profile
PEP	Power Elevation Profile
PLC	Programmable Logic Controller
POC	Proof-of-Concept
REST API	Representational State Transfer - Application Programming Interface
RMS	Root Mean Square
RT	Ray Trace
RTI	Real Time Industrial Bus/Application
RTT	Round Trip Time
SCADA	Supervisory Control And Data Acquisition
SLAM	Simultaneous localization and mapping
SW	Software

TCP	Transport Control Protocol
THz	Terahertz
UDP	User Datagram Protocol
VLC	Visible Light Communications
VR	Virtual Reality
WIET	Wireless Information and Energy Transfer

Executive Summary

The TIMES project is studying the use and potential of THz communications for industrial applications, and as part of the research, the project has described several industrial scenarios and use cases in manufacturing and logistics. In this context, the project has especially looked on how stationary production machines and moving robots need to communicate for an efficient and safe production process.

1 Introduction

This deliverable contains refinement and validation of identified scenarios and key performance indicators (KPIs). The aim of this task is to critically review, validate and update the initially adopted use cases and KPIs based on the findings from other WPs including channel measurements (WP3), technological enablers (WP4, WP5), and demonstrator development (WP6).
Contribution to this Deliverable come from ALL PARTNERS, that will provide updates based on their own activities and experience during the project.

1.1 Scope

This deliverable will document the continuous update process on scenarios and KPIs during the project. The scenarios and KPIs defined in the deliverable D2.1, D2.2, D2.3 will be confirmed and/or updated.

Inputs come from the work executed in WP3, WP4, WP5, WP6 and the output of this deliverable is used by WP6, WP7.

1.2 Audience

The main audience of this deliverable is the technology partners of the TIMES project, which will work on testing, simulations and developing components and devices for THz industrial communications.

1.3 Structure

The rest of the document is structured as follows:

- Chapter 2 contains critical comment to the activity and experience initially described and expected in D2.1 on *Industrial scenario and main project KPI*.
- Chapter 3 contains critical comment to the activity and experience initially described and expected in D2.2 on *Definition of scenario for Software Simulation and Simulation*.
- Chapter 4 contains critical comment to the activity and experience initially described and expected in D2.3 on *Definition of the scenarios and KPI for HW demonstration and PoC*

2 Critical Comment to D2.1 - Definition of use cases, KPIs, and scenarios for channel measurements

2.1 Critical Comment on USE CASES and KPI

This section will presents some critical comment and results on the applicability of 6G communication on the Industrial Use Cases and about the KPI needed for the industrial scenario

2.1.1 Comment on KPI request for Industrial application

During the development of Project Times, the technical specifications for the communication in Industrial environment have been confirmed, and the value on the table below are considered correct requirements for this kind of application. Below we present a short resume of the requirement listed in D2.1:

From D2.1 in *italic* below:

Each application may have varying standards for real-time, near-real-time, and non-real-time requirements, depending on the specific context. For industrial dynamic robots, stringent values are observed. To categorize industrial applications according to their link latency demands, we have devised a table that assigns them to three distinct categories: real-time, near-real-time, and non-real-time. D2.1 : Table 1 *acts as a reference for evaluating the link latency requirements of diverse industrial applications.*

D2.1 : Table 1 Real-time requirements terminology and definitions used in this report

Real-Time Requirement	Real Time	Near-Real Time	Non-Real Time
Link Latency	< 0.05 ms	0.05-5 ms	> 5 ms

We have incorporated a comprehensive range of throughput requirements, spanning from small to medium, high, and even ultra-high levels, as shown in D2.1 : Table 2*. However, given the complexity of industrial environments, which often involve numerous moving objects, we have assumed non-line-of-sight (NLOS) conditions, where direct light transmission may be obstructed.*

D2.1 : Table 2 Data rate terminology and definitions used in this report

Data Rate	Small	Medium	High	Ultra-High
Mean Throughput	< 50 Mbps	50-200 Mbps	200 Mbps - 1 Gbps	> 1 Gbps

These requirements have been used to classify the Industrial Use Cases in term of demanding needs in:

- **Latency**
- **Data Rate**

Maintaining this approach and considering the level of performance achieved during the Project Times, we can review and criticize the time of readiness of Use Case Classes.

The development of the radio devices showed that the main criticalities for the 6G communication in Industrial Environment are represented by:

- Many obstacles interposed along the radio wave beam
- High loss of radio beam during its propagation in industrial environment due to obstacles
- Low maturity level of intelligent RIS to use effectiveness the NLOS propagation (today far to be achieved)
- Big Dimension of radio/modem/antenna equipment, don't match with the assembly inside machine and match with assembly outside machine

The points above show that to use the 6G communication, with the Technology of today, the Industrial Environment must be:

- Open and without Obstacles -> suggest LOS communication or NLOS communication but between NON movable point
- Architecture based on use of concentrator of data -> many single CPU must communicate their data to a concentrator equipped with 6G Technology, and from this point the communication to a «twin» 6G point with the same characteristics starts.

Due to these considerations, and in particular to the points (1), (4), (5) all INTRA MACHINE applications can be excluded by the usage of this technology. The INTRA MACHINE communication can be done efficiently with Wired Gbit Ethernet communication and with Wired Fiber Optic communication, with some advantage for future development to increase the data rate using Fiber Optic Technology. The table below describes the applicability of 6G for the usage in INTRA or INTER Machine Communications.

Table 1 : 6G Applicability INTRA/INTER Machine

6G Application Usage	**Suggested Conclusion**	**Applicability**	
		Fixed Application	Movable Application
Intra Machine	NO : NOT Adeguate, NOT Suitable	NO	NO
Inter Machine	Could Be Used	Yes, but difficult	Could be done, high level of difficulty

About the KPI Target to use 6G Communication in the main Automation Industrial Application, the requirements remain the same as defined in D2.1 and reported in table below:

KPI	**Target**
Typical wireless user mean data rate (at half-max distance LoS connection, MAC layer)	LoS: up to 1 Tbps NLoS: > 100 Gbps

Reliability	LoS: 10^{-9} NLoS: 10^{-4}
L2 latency	RTI :50 μs NON RTI 200 μs
L2 jitter	RTI :1 μs NON RTI 2 μs
Localization accuracy (error standard deviation in the *x-y* plane)	LoS: 1 mm NLoS: < 10 cm
Localization latency	<1 ms
Area Traffic Capacity	>10 Gbps/ m^2

Today we are far from the Target Value and need to be redefine what have been achieved in the Project and what can be achieved in next 3/5 years, see the value achieved in POC1 in table below

D2.1 : Table 3 Network KPIs and target values for the TIMES THz system

KPI	Current 5G performance in mm-wave bands	Estimated KPIs of TIMES HW PoC	Estimated KPIs of scaled up TIMES networks
Typical wireless user mean data rate (at half-max distance LoS connection, MAC layer)	LoS: < 10 Gbps NLoS: 1 Gbps	LoS: < 10 Gbps NLoS[1]: 5 Gbps	LoS: up to 1 Tbps NLoS: > 100 Gbps
Reliability	LoS: 10^{-5} NLoS: 10^{-2}	LoS: 10^{-5} - 10^{-9} NLoS: 10^{-3}	LoS: 10^{-9} NLoS: 10^{-4}
L2 latency	> 0.5 ms	128 μs **500μs (achieved in POC1)**	RTI :50 μs NON RTI 200 μs
L2 jitter	> 0.25 ms	2 μs **6μs (achieved in POC1)**	RTI :1 μs NON RTI 2 μs
Localization accuracy (error standard deviation in the *x-y* plane)	LoS: 0.5 m NLoS: N/A	LoS: 1 cm NLoS: <0.5 m	LoS: 1 mm NLoS: < 10 cm
Localization latency	>10 ms	N/A	<1 ms
Area Traffic Capacity	10 Mbps/m^2	up to 10 Gbps/m^2	>10 Gbps/ m^2
THz-related KPIs: Sensing Resolution	N/A	N/A	1cm @ 1m

2.1.2 Comment on Industrial USE CASES

Based on the considerations in the previous section, "Comment on KPI request for Industrial application," all tables for the seven Industrial Use Cases have been reviewed. The first seven columns contain the original descriptions and values established at the beginning of the TIMES project; the last two columns represent the critical comments at the end of the project. The two right-hand columns in Table 2 contain critical comments written regarding the applicability and the time-to-completion for the use-case classes for THz communications. These comments can be grouped into three categories with respect to the time axis:

- Time to complete (2–3 years): The technology is mature enough, and standards already exist. With proper integration into chipsets, products can be developed. This applies specifically to fixed communication links.

- Time to complete (5 years): This timeframe covers use cases with moderate mobility, as demonstrated in PoC2 of the TIMES project. Some effort is required to bring these demonstrators to a higher TRL.

- Time to complete (> 5 years): This applies to use cases involving high mobility or real-time (RT) robotics and mechatronic controls. This area is not yet mature enough and requires significant research efforts.

Table 2 : Critical Review of Applicability of 6G in Industrial Use Cases

Description at the BEGIN of TIMES Prj.							**Critical Comment at the END of TIMES Prj.**	
Macro class	**Class description**	**Subclass**	**Specific use cases - subclass**	**Timeline in D2.1**	**Latency Req.**	**DataRate Req**	**Applicability**	**Time to Complete [years]**
A	Mobile Robot Management	A.1	Automated and guided vehicles and mobile robots + Offloading of localization and video processing operations for smart transportation vehicles	mid	⏳⏳⏳	**	NOT Today, Very difficult in the future	5
		A.2	Online cooperative high-resolution 3D map building	mid	⏳⏳⏳	**	NOT Today, Very difficult in the future	5
B	Predictive maintenance, monitoring of machine / Production line with Hi data Flow, substitute Field Bus in NON RTI Applications	B.1	Predictive Maintenance	mid	⏳⏳	***	YES in fixed position	2/3
		B.2	Monitoring - Video and Mechatronic Data +Remote access and maintenance	short/mid	⏳	****	YES in fixed position	5
		B.3	Process Automation + Connectivity for the factory floor	Mid	⏳⏳⏳	**	YES in fixed position	2/3

C	AR/VR - Digital Twin - Virtual Commissioning - Hi Level Maintenance	C.1	Virtual Simulation / Commissioning - AR + Maintenance in Factory and Warehouses	Mid	⌛⌛	**	YES in fixed position	5
		C.2	Ultimate immersive cloud VR/AR + Glass-free 3D and holographic displays	Mid	⌛⌛⌛	****	YES in fixed position	5
D	High Dynamic Control, Substitute Field Bus in RTI for Motion and Robotics	D.1	Substitution of RTI wired Buses with 6G wireless for Virtual PLC/EDGE + Motion control + Offloading of the PLC control function to the edge	Long	⌛	****	NOT Today, In Fixed Position in the Future	>5
		D.2	Control-to-control communication (motion subsystems) + ex of rotating machine	Long	⌛⌛	***	NOT Today, In Fixed Position in the Future	>5
		D.3	Motion Control + Seamless integration with Industrial Ethernet	long	⌛/⌛⌛	***	NOT Today, In Fixed Position in the Future	>5
E	Ensuring Seamless and Secure Field Bus Substitution Process	E.1	Mobile control panels with safety functions	long	⌛⌛⌛	**	NOT TODAY	>5
		E.2	Real-time cooperative safety protection	mid	⌛⌛⌛	**	NOT TODAY	>5
F	Flexible Factory	F.1	Flexible, modular assembly area + Factory of the future	long	⌛⌛	**	YES in fixed position	5
		F.2	Collaborative robots in groups + From intelligent robots to cyborgs	long	⌛⌛	**	NOT TODAY	>5

		F.3	Variable message reliability	mid	⧖⧖⧖	*	YES in fixed position	2/3

Legend for Table 2:

⧖⧖⧖=Not-RT; ⧖⧖=Near-RT; ⧖=RT – (RT means Real Time application)

*=Low data rate; **=Medium data rate; ***=High data rate; ****=Ultra-high data rate

⇨=Short term; ⇨⇨=Mid-term; ⇨⇨⇨=Long-term

In conclusion, the main obstacle today for the application of 6G in industrial environments comes from mobile NLOS (Non-Line-of-Sight) applications and the complex architecture of industrial environments, which presents many obstacles along the 6G radio beam.

2.2 Channel Sounder, Channel Measurement

2.2.1 Overview of Planned and Conducted Measurement Scenarios

The goal of the channel measurements conducted within the TIMES project was “to collect knowledge about the propagation behaviour of THz radio waves in industrial scenarios” [D2.1]. To achieve this goal, a scenario classification was defined, in which all scenario types were divided into two main groups: intra-device and inter-device. Two machine categories were considered, namely medium and large, with dimensions ranging from 1 to 100 m. The scenarios covered both static and dynamic conditions, where dynamic conditions refer to mobility introduced either by moving obstacles or by a moving Tx or Rx. In addition, scenarios including IRS in both intra-device and inter-device cases were introduced.

Tables below provide a list of the proposed measurement scenarios. The first six rows contain information included in D2.1, while the last row gives a conclusion indicating whether the scenario was measured, which results were obtained, and a reference to the corresponding TIMES document, including the page number where the scenario and its results are described in detail.

It can be seen that eight out of the nine planned scenario types were measured and analysed.

2.2.2 Intra-Machine scenarios

Scenario 1: Large machine; static conditions

Description:	Investigating the communication link between two nodes inside a large machine with few or no moving parts, to replace a cabled connection.
Links to use case:	E.g., predictive maintenance; substitution of wired RTI
Physical conditions:	LOS and NLOS
Tx-Rx distance:	1-10m
Mobility:	None (static)
Type of measurement	Limitations of wireless connections inside complex mechanical structures.
Conclusion in the End of TIMES	Reconstruction of connection between two SNs inside milling machine. Output: PAEP, PADP, DS, ASA, ESA, ASD, ESD. Details: D3.1, pp.46 – 48.

Scenario 2: Large machine; moving object

Description:	Investigating the communication link between two nodes inside a large machine with moving parts, to replace a cabled connection.
Links to use case:	E.g., predictive maintenance; substitution of wired RTI
Physical conditions:	LOS and NLOS
Tx-Rx distance:	1-10m
Mobility:	Yes, moving parts
Type of measurement	Limitations of wireless connections inside complex mechanical structures and how much moving parts in the propagation path affect the channel.
Conclusion in the End of TIMES	Not performed

Scenario 3: Large machine; IRS inside

Description:	Investigating the communication link between two nodes inside a large machine with few or no moving parts, to replace a cabled connection.
Links to use case:	E.g., predictive maintenance; substitution of wired RTI
Physical conditions:	NLOS
Tx-Rx distance:	1-10m
Mobility:	None (static)
Type of measurement	Investigate gain of installing IRS inside the machine to mitigate NLOS conditions and to improve the link performance in a complex mechanical structure.
Conclusion in the End of TIMES	Milling machine: Rx located inside machine, Tx outside. LOS link between Tx and Rx blocked by the machine door, IRS established the connection. Output: PDP, mean DS, rms DS. Details: D3.2, pp.22 – 26.

Scenario 4: Medium machine; static conditions

Description:	Similar to scenario 1; but smaller dimensions
Links to use case:	E.g., predictive maintenance; substitution of wired RTI
Physical conditions:	LOS and NLOS
Tx-Rx distance:	10 cm-100 cm
Mobility:	None (static)
Type of measurement	Limitations of wireless connections inside complex mechanical structures.
Conclusion in the End of TIMES	Reconstruction of connection between two SNs inside milling machine. Output: PAEP, PADP, DS, ASA, ESA, ASD, ESD. Details: D3.1, pp.46 – 48.

Scenario 5: Medium machine; moving object

Description:	Similar to scenario 2, but smaller dimensions
Links to use case:	E.g., predictive maintenance; substitution of wired RTI
Physical conditions:	LOS and NLOS
Tx-Rx distance:	10 cm-100 cm
Mobility:	Yes, moving parts (stationary Tx and Rx)
Type of measurement	Limitations of wireless connections inside complex mechanical structures and how much moving parts in the propagation path affect the channel.
Conclusion in the End of TIMES	Milling machine: fixed Tx and Rx, movement of the milling machine window from closed to completely open. Output: Rx power depending on the window gap. Details: D3.1, pp. 40.

2.2.3 Inter-Machine scenarios

Scenario 6: Medium machines; static conditions

Description:	Investigating the link can be established between an access point/base station and a sensor device. Communicating with a sensor or actuator outside or inside a machine.
Links to use case:	E.g., Wireless sensors and connection
Physical conditions:	LOS and NLOS
Tx-Rx distance:	10 m – 100 m
Mobility:	None (static)
Type of measurement	Propagation properties of the link outside the machine. Loss properties to reach inside a machine.
Conclusion in the End of TIMES	Milling machine inter-device: Rx located inside machine and Tx outside. Output: PG, DS, ASA, ESA, ASD, ESD. Details: D3.1, pp. 21 –22.
	Small industrial workshop: characterization of PL and large-scale parameters in LOS and NLOS settings. Output: CI and AGB model parametrization. Details: D3.1, pp. 17 – 21., @HWDU
	Access point scenario in big industrial hall, reconstruction of the AP on the wall communicated with SNs on machines. Output: PDP, PG, DS. Details: D3.1, pp. 26 – 33.

	Access point scenario scenario in robotic laboratory, reconstruction of the communication between AP and SNs on the robotic manipulators. Output: PDP, PG, DS. Details: D3.1, pp. 33 – 38.

Scenario 7: Medium machines; moving object

Description:	Same as scenario 6, but with a moving object in the propagation path. This can be a moving robot in a factory hall or moving humans.
Links to use case:	E.g., wireless sensors and connections, safety for operators,
Physical conditions:	LOS and NLOS
Tx-Rx distance:	10 m – 100 m
Mobility:	Yes, moving object (stationary Tx and Rx)
Type of measurement	Propagation properties of the link outside the machine. Dynamic behaviour of the channel due to environmental dynamics.
Conclusion in the End of TIMES	Two robotic arms communication with moving third arm between them, in case of different Tx height. Two movement type: vertical (up and down) and rotational. Output: time-variant PDP and PG. Details: D3.1, pp.40 – 42.

Scenario 8: Medium machines; moving Tx or Rx

Description:	Investigating the communication between an access point and a robot or other moving object in a factory /production environment. This can be a moving robot, a moving part on a stationary machine, or even a human operator.
Links to use case:	E.g., Mobile robots; safety for operators
Physical conditions:	LOS
Tx-Rx distance:	10 m – 100 m
Mobility:	Yes, moving Tx or Rx
Type of measurement	Propagation properties of the link outside machines. Dynamic behaviour of the channel due to mobility.
Conclusion in the End of TIMES	Access point with moving Rx and fixed Tx in big industrial hall. Output: time-variant PDP and PG. Details: D3.1, pp.43 – 46.

Scenario 9: Medium machines; IRS to mitigate propagation loss

Description:	Similar to scenarios 6 and 8. Investigating the communicating with a sensor or actuator outside a machine, or with a moving robot and the benefits of using IRS in the environment.
Links to use case:	E.g., Mobile robot; wireless sensors and connections
Physical conditions:	NLOS
Tx-Rx distance:	10 m – 100 m
Mobility:	Static measurements
Type of measurement	Investigate how an IRS installed in the factory environment can improve the propagation channel and path loss in NLOS situations

Conclusion in the End of TIMES	Azimuthal scanning measurements in robotic laboratory: Tx and Rx fixed, with blocked LOS linked (massive concrete obstacle), connection possible due to IRS. Measurements included three setups with different Tx, Rx, IRS locations. Outputs: PAP, ASA AoD, ASA AoA. Details: D3.2, pp.17 – 22.

3 Critical Comment to D2.2 - Definition of scenarios for software

3.1 Models and parameters for wireless nodes

In D2.2, we defined the simulation models and parameters for the modeling of wireless nodes. Due to the limited availability of empirical evidence at that stage of the project, these parameters were defined based on literature review, practical design considerations, and discussions during task and consortium meetings. Two device categories were introduced, namely low-end and high-end nodes, in order to capture different levels of hardware complexity and performance capabilities.

In the present deliverable, we revisit our initial assumptions and update the simulation parameters in light of the latest technological developments in the THz domain and the results of the empirical evaluations conducted using the THz devices developed within WP5.

This section provides a critical assessment of the initially defined modeling parameters, evaluating their consistency with the experimental evidence and implementation constraints observed during the project. Where discrepancies are identified, updated parameter values and modeling assumptions are proposed to ensure alignment with the validated technological capabilities.

In Table 3, the simulation parameters defined in D2.2 are reported, and a critical analysis is provided below.

Table 3: Simulation parameters defined in D2.2.

Symbol	Parameter	Device Type	
		Low-end	**High-end**
	Transmit power	-10 to 0 dBm [21] [22]	Up to 25 dBm [23]
NF	Noise Figure	10-15 dB [24]	8 dB [23]
$G_{Tx/Rx}$	Antenna gains	6 dBi [23]	Up to 55 dBi [25]
-	Frequency range	0.2 to 1.5 THz	
B	Bandwidth	Starting from 0.5 GHz [26], up to 2.16 GHz [23]	Up to 100 GHz [26]
-	Modulation type	OOK [23], PPM [27], BPSK [23]	8-PSK, *M*-QAM | *M*=4,16,64 [23]
	FFT size	64, 128	{256 [28], 512, 1024, 2048, 3168 [29], 4096 [30]}
	No. of transceiver chains	Up to 256	
	Antenna array size	{1,2,4,6,20} [31]	16 by 16 [32]
	Beam-switching time	10 ns	

Regarding the simulation parameters listed in Table 3, several updates have been introduced based on the measured and characterized radio-frequency (RF) impairments. The transmit power values were determined

according to the measured performance of an InGaAs mHEMT power amplifier (PA) operating in the 270–330 GHz band [1]. The achievable transmit power ranges between approximately -2.5 dBm and 4.6 dBm, depending on the selected center frequency [2]. These values assume the presence of a digital pre-distortion (DPD) block at the transmitter.

Further analysis revealed pronounced memory effects in the PA, which showed a clear dependence on the adopted channel bandwidth and waveform structure. In particular, it was observed that even in the presence of DPD, multi-carrier waveforms, specifically orthogonal frequency division multiplexing (OFDM), exhibit inferior performance compared to single-carrier waveforms, especially for bandwidths exceeding 2.16 GHz, which corresponds to the smallest bandwidth defined in the IEEE 802.15.3d standard.

The antenna gain values reported in Table 3 are consistent with those achieved by the real prototypes developed within the project. As reported in [3], the fixed high-directivity lens-coupled horn antenna achieved a directivity of 50.5 dBi with losses below 1 dB. In contrast, the steerable leaky-wave and phase delay line antennas exhibit a directivity of approximately 20 dBi, with losses of 13 dB and 17 dB, respectively, resulting in total gains of 7 dB and 3 dB.

Regarding the FFT size, the most significant degradation in error performance from the PA perspective occurs when transitioning from single-carrier transmission to OFDM. However, within OFDM systems, increasing the FFT size itself has only a marginal effect on the overall error performance [2].

From the oscillator phase-noise perspective, increasing the FFT size while keeping the total bandwidth fixed reduces the subcarrier spacing, thereby increasing the sensitivity of the system to phase noise. Under such conditions, phase tracking reference signals (PTRS) are required to continuously track and compensate for the phase variations of the received signal.

3.2 Critical comments on MIMO simulation scenarios

In D4.1 (Sect. 2) and D4.3 (Sect. 2), the performance of a massive MIMO system operating in the sub-THz band is evaluated through MATLAB-based simulations. While channel state information (CSI) is assumed to be perfect in the former, the latter extends the analysis to a more practical scenario of imperfect CSI.

Most simulation parameters are aligned with those specified in D2.2; however, some deviations are introduced. These differences are discussed below:

- MIMO systems achieve performance gains primarily through the coherent combination of signals transmitted and received across multiple antennas. Consequently, precoding and combining vectors play a more critical role in determining system performance than antenna directivity. For this reason, both the base station (BS) and all user equipment (UEs) are assumed to use isotropic antennas, meaning each antenna has uniform gain in all directions. Each UE is equipped with a single antenna, while the BS employs a uniform planar array consisting of hundreds or even thousands of antennas.
- To evaluate the feasibility of a 1 Tbps throughput in line-of-sight (LoS) environments, reported in D2.1, a LoS channel model is assumed.
- To avoid excessively low per-antenna signal-to-noise ratio (SNR) at the edge of the service area, a minimum UE transmit power of 0 dBm is assumed.
- To account for future hardware advancements, a performance benchmark is established under forward-looking assumptions in D4.1 (Sec. 2): a maximum UE transmit power of 30 dBm, a BS equipped with either 1024 or 4096 antennas, and a fully digital architecture.

- The benchmark performances from D4.1 (Sec. 2) are evaluated under more realistic assumptions in D4.3 (Sec. 2). Specifically, to limit power consumption, a hybrid architecture is adopted instead of a fully digital one; consistently with the capabilities of a high-end device, reported in Table3, the BS deploys 256 antennas; and each UE transmit with a power of 15 dBm.

Both D4.1 (Sec. 2) and D4.3 (Sec. 2) report encouraging results, showing that THz communications can significantly outperform traditional RF systems up to the mmWave bands due to enhanced beamforming and spatial multiplexing gains. Notably, a theoretical throughput of 1 Tbps is obtained under both ideal conditions (D4.1) and more realistic scenarios (D4.3). However, we must be aware that achieving such high data rates requires aggregating the traffic of a high number of UEs, which is only practical for limited use cases. Moreover, the BS must handle the substantial total received power from simultaneous UE transmissions, which remains a key challenge.

3.3 Simulation scenarios and tools for software simulations

In the initial phase of the project (D2.2), a candidate set of simulation scenarios and tools was identified as most suitable to support the analysis of the selected use cases and KPIs. These recommendations were based on the expected modeling requirements, including THz channel characterization, and system- and link-level performance evaluation.

In this section, we reassess our initial choices in light of the experience gained during the project. In particular, we evaluate whether the recommended tools effectively supported the activities across WPs, or whether alternative platforms and frameworks proved more appropriate in practice. The analysis highlights the lessons learned, the limitations encountered, and any adjustments made to the simulation workflow to ensure consistency with experimental results and demonstrator developments.

3.3.1 Ray-tracing simulations

In D2.2, several ray-tracing (RT) tools were analysed and compared based on the requirements of the project. Among them, SiMoNe and Sionna RT were identified as the most suitable candidates. At that time, Sionna RT had not yet been fully validated for simulations at THz frequencies. However, subsequent evaluations carried out within the context of this project demonstrated its applicability to THz ray-tracing simulations [4, 5]. In addition, a third tool, 3DScat, which was not originally considered in D2.2, was later adopted and used within the project. In the following, we summarize the main motivations for the selection of each tool and how they have been used in the project.

Sionna RT

Sionna RT was used to carry out activities in WP3 and WP4. In WP3, it was employed to analyse the second-order statistics of industrial THz channels. For this purpose, simulations were performed using the digital model of the BiRex Pilot Plant presented in D2.2. The simulations considered different clutter densities by placing varying numbers of mobile robots within the scenario. In WP4, Sionna RT was used to emulate blockage scenarios in industrial environments. In this case as well, the digital model of the BiRex Pilot Plant was adopted, and multiple simulations were conducted with moving robots acting as blockers and following different trajectories. Sionna RT was selected for these studies because it enables flexible and easy configuration of obstacles and moving objects, a capability that is not available in other tools such as SiMoNe and 3DScat.

SiMoNe

SiMoNe ray tracing tool was chosen since it supports RIS-assisted channel ray tracing and allows the integration of realistic RIS, Tx, and Rx radiation patterns together with a 3D model of the measurement environment. In WP3, it was used to recreate the RIS-assisted measurement scenarios described in TIMES D3.2 and to verify the implemented RIS ray tracing approach by direct comparison with measurement results. For this purpose, the RIS radiation pattern provided by the partners who designed the prototype, as well as the antenna patterns and the environmental model, were incorporated into the tool. The comparison showed that SiMoNe provides generally reliable results, especially for estimating power gain improvements and studying the effect of different RIS configurations, although the accuracy strongly depends on the quality and validity of the input data, particularly the RIS radiation pattern. Overall, the study confirmed that, with proper input data, SiMoNe RIS-assisted ray tracing is an efficient and scalable tool for the design and evaluation of RIS-assisted communication systems. In WP4, the SiMoNe ray tracing tool was further used to evaluate the placement of RIS in the considered industrial scenario of the TIMES PoC. Based on a 3D model of the AETNA Robopac factory environment, ray tracing simulations were performed to estimate the path loss for different Tx, Rx, and RIS positions. The obtained path loss predictions were then used to derive feasible deployment configurations and to estimate the achievable data rates of RIS-assisted links. This analysis served as a basis for selecting suitable RIS and node placements for the experimental PoC setup.

3DScat

The third tool adopted to perform signal propagation simulations is 3DScat. This tool was selected to obtain a realistic channel representation and reliable results at THz frequencies, where accurate modeling of propagation phenomena becomes particularly critical. Unlike other tools, the 3DScat RT adopts a geometric modeling approach that combines the principles of ray theory with diffraction and diffuse scattering models. This tool has a lot of degrees of freedom and allows to specify each detail of the scenario and simulation. These include the environmental layout, the material composition of objects (i.e., facility, obstacles, furniture), and the number and types of interactions considered in the simulation (e.g., reflection, diffraction, and scattering). The electromagnetic properties of materials affecting signal propagation are modelled through parameters including the relative dielectric constant and the electrical conductivity. Another relevant capability of the tool is the support for reconfigurable intelligent surfaces (RIS), which can be modelled as either anomalous reflectors or focusing lenses.

Within the scope of this project, the RT tool was used to analyze signal propagation in diverse industrial environments including AETNA Robopac and the Bi-Rex pilot line. In particular, it enabled the comparison of THz communication performance with that observed at lower frequency bands such as sub-6 GHz and mmWaves. The simulations were conducted for different communication configurations, including base station-to-node and node-to-node links, considering both fixed devices and mobile nodes such as automated guided vehicles (AGVs). In addition, the tool was employed to generate a labeled dataset used to support channel modelling approaches based on machine learning techniques aimed to extrapolate the main channel parameters such as path loss exponent and the standard deviation of shadowing [7]. Finally, the simulator was exploited to evaluate the potential performance improvements enabled by the deployment of RIS, both locally and in a global scale, and to derive general guidelines for RIS placement and configuration under different operational modes and industrial use cases [6].

3.3.2 System-level simulations

In D2.2, SiMoNe and ns-3 were identified as the most suitable simulation tools for conducting system-level simulations. It was anticipated that both simulators would require modifications to support the evaluation

of the solutions developed within the project. Ultimately, SiMoNe was adopted, as the use of ns-3 would have required a higher development effort. In addition, custom simulators were developed to address specific requirements related to THz multi-hop networks and the AI-driven optimisation approaches targeted by the project.

SiMoNe system-level simulator

The SiMoNe system-level simulator was used to analyze the behavior of the beam alignment and tracking approach based on leaky wave antennas (LWAs) in mobile communication scenarios. For this purpose, the simulator was extended to support the specific characteristics of LWAs, in particular their frequency-dependent beam steering behavior. This extension enabled the modeling of handover procedures where changes in carrier frequency correspond to changes in beam direction. Within this framework, system-level simulations were conducted to investigate the influence of key parameters of the handover procedure, including the update interval of the beam alignment mechanism and the angular estimation error of the user position. These simulations were used to support the design and parameterization of the handover procedure required to maintain reliable connectivity during user mobility.

Custom Simulation Tools for Network Optimizations for THz-based systems in industrial environments

To support the research activities on THz networking and intelligent network management, two custom simulation tools were developed. These tools were designed to provide high flexibility in protocol design, integration with advanced physical-layer models, and rapid experimentation with AI-based algorithms. While widely adopted network simulators such as SiMoNe, ns-3[1] and OMNeT++[2] provide extensive functionality, the specific requirements of THz multi-hop networks and AI-driven optimization motivated the development of lightweight and highly customizable simulation environments.

The first tool was developed to support the activities “MAC and routing protocols design in multi-hop THz networks” and “AI-based MAC optimization for multi-goal scenarios,” reported in deliverable D4.4 [8].

It consists of a Python-based network simulator implementing a hybrid simulation paradigm combining time-driven and event-driven approaches. In this framework, the simulator models packet transmissions between user devices and base stations, as well as user-to-user communications, following a discrete temporal flow. However, when no relevant events occur for several time instants, the simulator advances the internal clock by skipping idle intervals. This hybrid mechanism preserves temporal fidelity while significantly reducing computational overhead compared to purely time-stepped simulations.

The simulator includes faithful implementations of the Aloha and CSMA/CA MAC protocols, which were specifically adapted to operate in THz frequency bands. The operating frequency is provided as an input parameter, and the simulator explicitly models propagation delays, which become relevant at THz frequencies due to the extremely high data rates and short transmission times. These protocol implementations allow accurate analysis of medium access behavior in multi-hop THz networks. The framework integrates custom channel models developed within the project together with standardized models derived from 3GPP specifications, enabling realistic propagation modeling across different scenarios.

The simulator accepts generic network layouts as input. In the project, these layouts were used to reproduce industrial environments such as the BIREX and AETNA facilities. Different traffic models can be simulated, allowing the evaluation of heterogeneous communication workloads typical of industrial and IoT deployments.

[1] https://apps.nsnam.org/app/thz/
[2] https://omnetpp.org/

The simulator produces a wide range of performance metrics, including, but not limited to:

- per-user throughput
- aggregate network throughput
- per-user latency
- average network latency
- packet drop ratio

These metrics enable detailed performance evaluation of MAC protocols, routing strategies, and AI-driven optimization mechanisms.

The second custom tool was developed within the activity "Predictive network management and RIS configuration via radar-based sensing," also reported in deliverable D4.4 [8].

This framework extends the previously described network simulator by introducing a network–physical layer co-simulation architecture, as illustrated in the following Figure:

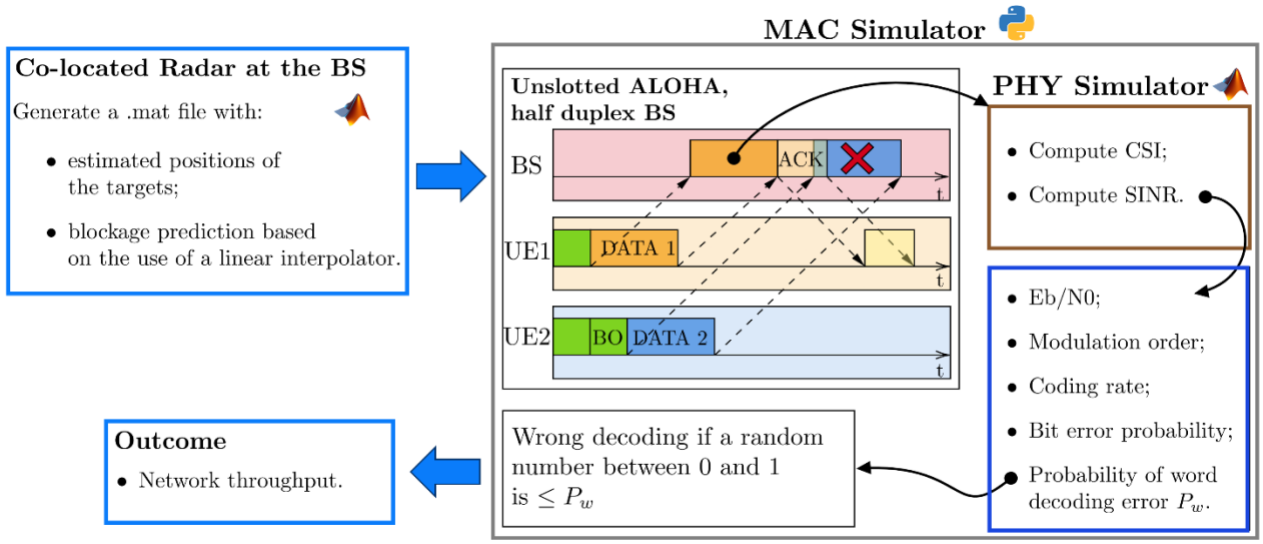

Figure 1: Block scheme of the custom Python-Matlab simulator

In this approach, the custom Python-based simulator described above continues to handle the MAC and network-layer logic, while the physical-layer propagation and signal modeling are computed using a dedicated Matlab simulation program. Instead of relying on conventional channel models, the Matlab component performs a detailed electromagnetic propagation simulation capable of computing received signal power contributions at the level of individual antenna elements and individual elements of the Reconfigurable Intelligent Surfaces (RISs) deployed in the scenario (whose position is an input of the simulator). This enables the simulation of multiple RIS architectures and different electromagnetic propagation models.

For each packet transmission event generated by the network simulator, the system invokes the Matlab physical-layer simulation to compute the resulting Signal-to-Interference-plus-Noise Ratio (SINR). The calculated SINR is then fed back into the network simulation to determine packet decoding success or failure. This tight coupling between network-layer dynamics and detailed electromagnetic modeling enables accurate evaluation of RIS-assisted communication strategies, as well as algorithms for predictive network management based on radar sensing and environmental awareness.

Although powerful simulation frameworks such as ns-3 and OMNeT++ offer extensive protocol libraries and realistic networking stacks, several technical considerations motivated the development of dedicated simulators for this project.

1. Rapid prototyping of low-level protocol mechanisms

The custom Python framework enables faster implementation and modification of low-level networking components compared to large C++-based simulation platforms. This is particularly advantageous when experimenting with:

- new routing protocols for multi-hop THz networks
- custom MAC adaptations for extremely high-frequency operation
- reinforcement learning and deep reinforcement learning (DRL) algorithms for network optimization
- radar-based localization and prediction algorithms integrated into network control

The simplified architecture significantly reduces development time when iterating on protocol designs.

2. Seamless integration with AI and data-driven algorithms

The simulator was designed with native compatibility with the Python ecosystem, enabling straightforward integration with machine learning libraries (e.g., reinforcement learning frameworks, optimization libraries, and data analysis tools). This is essential for evaluating **AI-based MAC optimization strategies** and other learning-based network control techniques.

In contrast, integrating advanced AI pipelines within traditional simulators often requires complex bindings or external interfaces.

3. Flexible parameterization and configuration

The custom framework provides extensive flexibility in defining simulation parameters, including:

- operating frequency (up to THz bands)
- propagation models
- node densities and deployment geometries
- traffic generation models
- MAC protocol parameters
- routing strategies

This flexibility is particularly valuable when exploring emerging **THz communication scenarios**, which are not yet fully supported by mainstream network simulators.

4. Efficient hybrid simulation strategy

The hybrid time-driven/event-driven execution model reduces computational cost while maintaining accurate timing behavior. This is especially beneficial in scenarios characterized by **bursty traffic patterns** or **sporadic communication events**, where purely time-stepped simulations would waste significant computation on idle intervals.

5. Tight coupling with advanced physical-layer simulations

The second tool enables a **fine-grained co-simulation between network and electromagnetic propagation models**, which would be difficult to achieve efficiently in traditional frameworks. The ability to invoke detailed Matlab simulations for each packet transmission allows accurate evaluation of:

- RIS-assisted links
- element-level beamforming effects
- radar-assisted environmental sensing

This level of physical-layer detail is rarely available in standard network simulators.

6. Simplified experimentation workflow

The lightweight architecture makes it easier to run large experimental campaigns, modify scenarios, and integrate new models without the overhead of maintaining a full-scale simulator environment. This facilitates rapid testing and iterative design.

7. Improved transparency and controllability

Because the simulation stack was developed specifically for the project, every component, from MAC timing to propagation modeling, is fully transparent and directly modifiable. This avoids hidden implementation assumptions that may exist in large pre-existing frameworks.

3.3.3 Link-level simulations

In D2.2, we identified SiMoNe as the most suitable tool for carrying out link-level simulations in the context of this project.

SiMoNe link-level simulator

In particular, SiMoNe was used to evaluate THz communication links employing LWAs for beam alignment and tracking. In these simulations, the physical layer of the communication system was modeled, including modulation, coding, and noise effects, in order to assess the link performance under realistic conditions. In particular, the achievable data rates were analyzed as a function of the path loss expected in the considered deployment scenarios. Furthermore, multicarrier simulations were conducted to study potential interference effects between adjacent carrier frequencies used for frequency-dependent beam steering with LWAs. The obtained simulation results were subsequently used to support the development and parameterization of the handover procedure required for beam alignment and tracking in mobile scenarios.

Custom link-level simulations with MATLAB

Additional link-level evaluations were carried out using custom MATLAB simulations. MATLAB was selected due to its high flexibility and its ability to support rapid implementation and evaluation of PHY-layer blocks. In contrast, implementing new solutions within SiMoNe would have required a significantly higher development effort

References

[1] L. John, A. Tessmann, A. Leuther, P. Neininger, and T. Zwick, “Investigation of Compact Power Amplifier Cells at THz Frequencies using InGaAs mHEMT Technology,” in 2019 IEEE MTT-S International Microwave Symposium (IMS), pp. 1261–1264, 2019.

[2] L. Samara, S. Haussmann, E. Tufa, A. A. D'Amico, T. Zugno, I. Kallfass, and T. Kürner, "Sub-THz Power Amplifiers: Measurements, Behavioral Modeling, and Predistortion Algorithms," IEEE Transactions on Terahertz Science and Technology, 2025.

[3] TIMES Deliverable D5.3, "Design fabrication and verification of high directivity and beam steering antennas at THz frequencies," 2025.

[4] S. Pahlke, T. Zugno, M. Boban, D. Dupleich and T. Kürner, "Ray Tracing and Measurement-Based Characterization of Inter/Intra-Machine THz Wireless Channels," 2024 18th European Conference on Antennas and Propagation (EuCAP), Glasgow, United Kingdom, 2024, pp. 1-5, doi: 10.23919/EuCAP60739.2024.10501627.

[5] D. Dupleich, D. Sitdikov, A. Ebert and M. Boban, "Measurement-based Validation of Ray-tracing Model at sub-THz for ISAC Applications of Blockage in Industrial Scenario," 2024 4th URSI Atlantic Radio Science Meeting (AT-RASC), Meloneras, Spain, 2024, pp. 1-4, doi: 10.46620/URSIATRASC24/MKTB3572.

[6] A. Tarozzi, E. M. Vitucci, F. Fuschini and R. Verdone, "Guidelines for RIS Planning in IIoT Scenarios," 2024 IEEE 8th Forum on Research and Technologies for Society and Industry Innovation (RTSI), Milano, Italy, 2024, pp. 488-493, doi: 10.1109/RTSI61910.2024.10761677.

[7] TIMES Deliverable D3.4, "Final Report on Channel Models for industrial environments at sub-THz frequencies," 2025.

[8] TIMES Deliverable D4.4, "Final report on multi-goal mesh network optimization and exploitation of smart propagation environments," 2025.

4 Critical Comment to D2.3 - Definition of the scenarios and KPI for HW demonstration and PoC

4.1 Overall outcome of the PoCs

As discussed in the TIMES deliverable D6.4, the final outcome of the PoCs is the following:

For PoC1, the final scenario has been validated. We were quite close at the end to the limit of the system in QAM-16, whereas we kept some margin in QPSK, and in any case, the performances required for the demo at AETNA were high enough. KPIs were assessed during the final demo, and were more or less in line with the estimated values from the starting of the project.

For PoC2, the initial scenario including the reconfigurable RIS and leaky-wave antenna was not fully validated. First, the R-RIS was found to have higher losses than expected, most probably due to the liquid cristal (LC) material that has losses at 300 GHz. TO go ahead, analysis of the material dielectric response, index and losses would be mandatory for future re-design of the R-RIS. However beyond the losses of the R-RIS, the reconfigurable status of the R-RIS was measured in the VNA at CNRS, confirming the design, at least for the index change part.

Hereafter, we remind some of the main outcomes and lessons learned related to the TIMES hardware built for the PoCs

4.1.1 THz Front ends

In the project it was planned to develop THz modules, consisting of a low-cost single package that is mounted on a back-end (BE) carrier as illustrated in Fig. 1. During the project it was decided to switch to classical waveguide modules, due to their superior performance in terms of output power and noise performance. The waveguide package incorporates the millimeter-wave monolithic integrated circuits (MMICs) and the relevant components and interfaces for the control of the LO signal as well as the bias control of the THz circuits. In Fig. 2 and 3 the TIMES modules including a simplified block diagram is depicted.

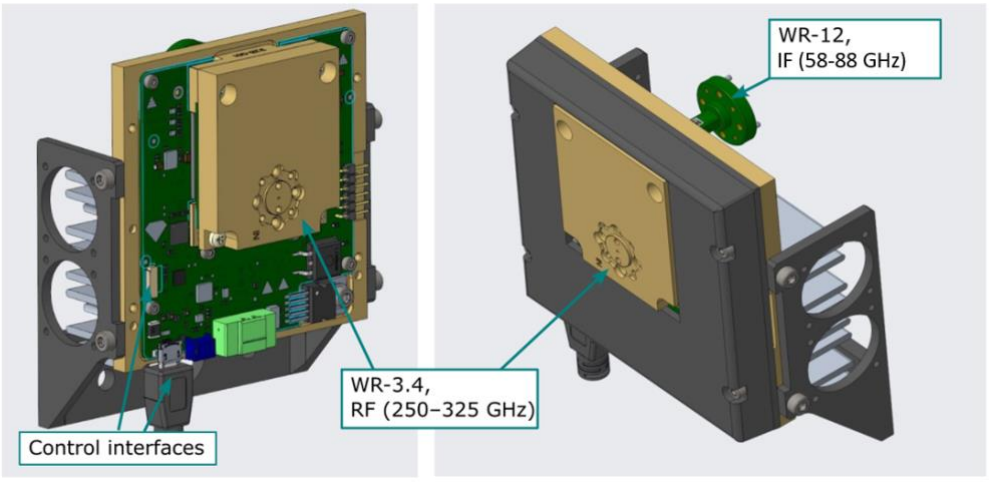

Fig. 1: Preliminary drawing of the 300-GHz FE modules.

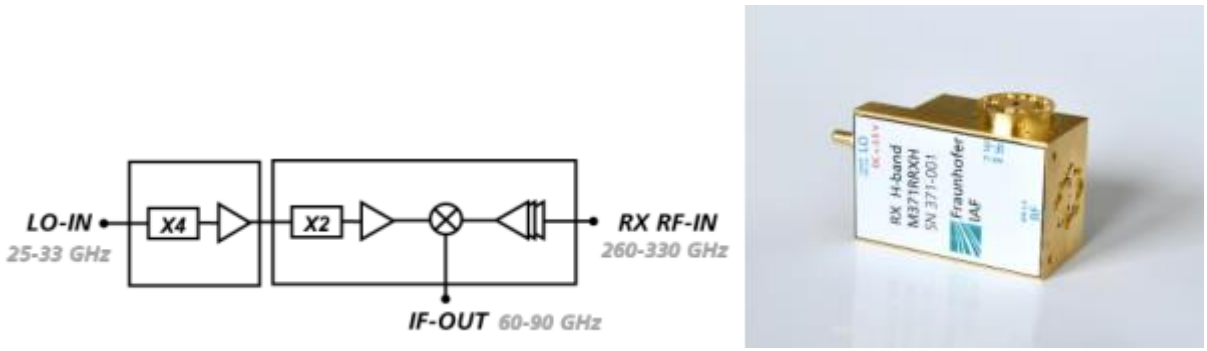

Fig. 2: Receiver block diagram (left) and the corresponding module (right).

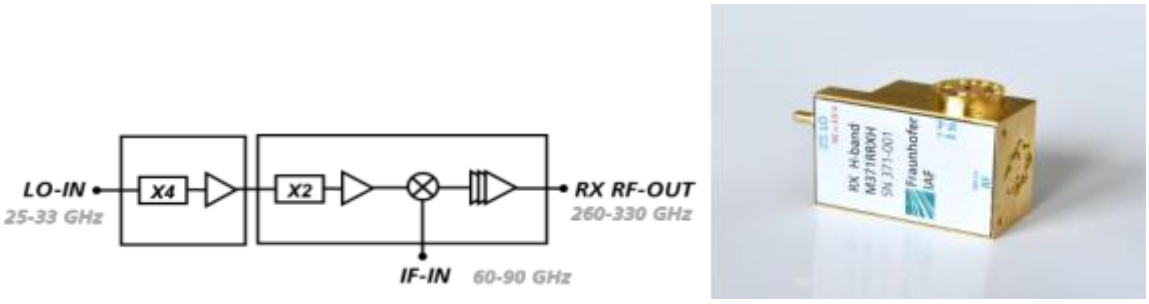

Fig. 3: Transmitter block diagram (left) and the corresponding module (right).

The targeted RF frequency range is 250 to 325 GHz, using the standard WR-3.4 waveguide flange. The IF frequency range has to cover the frequency bands of the TDD and FDD modem frequency ranges, which is approximately 58 to 88 GHz, compliant to the WR12 range. All relevant interfaces are listed in the table below.

Interface specifications RX/TX modules	
RF frequency range (GHz)	250 … 325
RF WG flange	WR-3.4
IF frequency range (GHz)	58 … 88
IF WG flange	WR-12

Tab. 4: General specifications of the Rx/Tx modules.

The only difference between the RX and TX modules are the integrated up- and downconverter circuits. The package dimensions, interfaces and positions of the interfaces are identical for both the RX and TX modules. The electrical specifications, like input and output power level of the RX and TX modules, are summarized in the following subsections.

Tx (up-converter) MMIC

Electrical specifications TX	Achieved	Predefined in D2.3
RF frequency range (GHz)	275 … 325	250 … 325
RF output power (dBm, OP1dB)	>0	> 3

IF frequency range (GHz)	<60 … >90	58 … 88
IF input power (dBm, IP1dB)	-20…-10	-15 … -5
IF input power (dBm, damage)	5…10	5 … 10

Tab. 5: General specifications of up-converter MMIC.

Tx (up-converter) Module

Electrical specifications TX	Achieved	Predefined in D2.3
RF frequency range (GHz)	270 … 325	250 … 325
RF output power (dBm, OP1dB)	0	> 6
IF frequency range (GHz)	<60 … >90	58 … 88
IF input power (dBm, IP1dB)	-10 … 0	-5 … 0
IF input power (dBm, damage)	5 … 10	5 … 10

Tab. 6: General specifications of the up-converter module.

The predefined specifications of the Tx from D2.3 could be well meet. As shown in Table 2 and 3, the required IF and RF bandwidths and frequency ranges are adequately covered, although the MMICs' operating range is shifted slightly toward higher frequencies owing to the onchip amplifier's frequency offset. Required power levels are nearly attained; however, the specified output power cannot be reached precisely because the amplifier's 1dB compression point (OP1dB) is lower than anticipated. To compensate for this limitation, an additional poweramplifier module is incorporated into the indoor units (IU) (see Section 6.3).

4.1.2 Power Amplifier Module

The Medium Power Amplifier Module (MPA) is responsible for providing sufficient output power to enable reliable high-data-rate communication links in the targeted frequency range of 260–320 GHz. It is designed to operate efficiently within the overall transceiver architecture while preserving broadband performance and spectral integrity.

Performance Characteristics

The MPA is designed to deliver an output power exceeding 10 mW across the operating band, fulfilling the requirements for THz wireless links.

Key performance features include:

- Broadband gain over the 260–320 GHz frequency range,
- High power density enabled by advanced mHEMT technology,
- Stable operation under varying bias conditions,
- Efficient scaling of output power with drain voltage.

Small-signal characterization confirms a flat gain response, while large-signal measurements demonstrate robust output power performance and predictable behavior under compression. These characteristics validate the suitability of the MPA for integration into high-performance THz transmit chains.

Biasing and Stability Considerations

The amplifier employs a dedicated biasing architecture that separates DC and RF paths. This strategy:

- Prevents interference between bias networks and RF signals,
- Reduces the risk of oscillations,
- Enables flexible bias tuning for performance optimization.

The use of vertical bias interconnects shortens current return paths and minimizes parasitic inductances, contributing to improved stability and reproducibility. This is particularly critical at THz frequencies, where even small parasitic effects can significantly impact performance.

Integration into the Front-End

Within the Indoor Unit, the MPA is positioned in the transmit chain after the frequency up-conversion stage. The upconverted THz signal is routed through a short waveguide interconnect to the amplifier module, minimizing insertion losses and preserving signal quality.

The amplified signal is then delivered to the RF output port, ensuring sufficient radiated power for system-level operation. The integration strategy emphasizes:

- Minimal interconnect length,
- Efficient thermal coupling to the module housing,
- Compatibility with the modular system architecture.

The MPA can also be operated as an independent module, allowing standalone characterization and flexible system configurations.

Packaging and Assembly

The MPA is assembled in a CNC-milled, gold-plated waveguide housing, consistent with the packaging approach used for the Tx and Rx modules. This packaging strategy provides:

- Low-loss RF transitions,
- Excellent electromagnetic shielding,
- Robust thermal management.

In contrast to multi-port front-end modules, the MPA integrates on-chip waveguide transitions, eliminating the need for additional probe substrates and reducing assembly complexity. This results in:

- Lower transition losses,
- Improved reproducibility,
- Simplified manufacturing.

The mechanical design ensures precise alignment of waveguide interfaces and stable electrical contact, both essential for reliable operation at THz frequencies.

Thermal Management

Due to the high power density of the amplifier, effective thermal management is essential. Heat generated within the MMIC is dissipated through:

- The chip mounting pedestal,
- The metallic waveguide housing acting as a heat sink,
- Direct thermal conduction paths to the module body.

This passive thermal management approach ensures stable operation without requiring active cooling, while maintaining compact system dimensions.

Electrical specifications HPA Module	Achieved	Predefined in D2.3
RF frequency range (GHz)	260-320	275 … 320
RF output power (dBm, OP1dB)	>7	>5
Gain (dB)	20	20

Tab. 7: General specifications of the up-converter module.

The Power Amplifier Module constitutes a high-performance, broadband THz amplification solution, combining advanced semiconductor technology with an optimized circuit and packaging approach. Its ability

to deliver stable output power, maintain spectral integrity, and integrate seamlessly into the transceiver architecture makes it a key enabler for practical THz communication systems

Rx (down-converter) MMIC

Electrical specifications RX	Achieved	Predefined in D2.3
RF frequency range (GHz)	270 … 325	250 … 325
RF input power (dBm, IP1dB)	-35 … -20	-30 … -20
RF input power (dBm, damage)	> -10	> - 15
IF frequency range (GHz)	<60 … >90	58 … 88
IF output power (dBm, OP1dB)	-22 … -8	-18 … -13

Tab. 8: General specifications of the down-converter MMIC

Rx (down-converter) Module

Electrical specifications RX	Achieved	Predefined in D2.3
RF frequency range (GHz)	280 … 325	250 … 325
RF input power (dBm, IP1dB)	-35 … -20	-30 … -20
RF input power (dBm, damage)	> -10	> - 15
IF frequency range (GHz)	<60 … >90	58 … 88
IF output power (dBm, OP1dB)	-25 … -10	-18 … -13

Tab. 9: General specifications of the down-converter Module

The predefined specifications of the Rx from D2.3 could again be well meet. As depicted in Table 7 and 8, the required IF and RF bandwidths and frequency ranges are adequately covered. As for the Tx, the Rx also shows a frequency shift in the operational frequency range towards higher frequencies, which can again be explained considering the offset also observed for the on-chip low noise amplifier. The required power levels were nearly achieved. The general performance of the MMIC front end chip sets is reported in [9]

4.1.3 Local oscillator specifications

The performance of the local oscillator (LO) subsystem is a critical enabler for the overall functionality of the THz front-end, directly impacting frequency accuracy, spectral purity, conversion gain. Within the TIMES THz front-end architecture, the LO signals are generated by dedicated PLL-based synthesizers and distributed separately to the transmit (Tx) and receive (Rx) paths, ensuring full-duplex operation with independent frequency control.

Frequency Range and Tuning Capability

The LO subsystem is designed to cover a frequency range of 24 GHz to 33.6 GHz, which is subsequently upconverted through frequency multiplication stages to support THz operation in the 275–325 GHz band. To enable flexible system operation and channel selection, the LO frequency is:

- Digitally tunable via a PLL synthesizer,
- Adjustable with discrete frequency steps, allowing deterministic frequency planning,
- Accessible through both software control (SPI/USB interface) and hardware stepping (Up/Down interface).

A predefined frequency grid ensures consistent and repeatable operation across the band, supporting system-level requirements such as frequency hopping, calibration, and channel allocation.

Output Power and Drive Requirements

The LO output power is specified in the range of 3 dBm to 7 dBm, ensuring sufficient drive level for the subsequent frequency multiplier stages and mixer circuits.

Amplitude control is implemented through a variable gain amplifier (VGA) stage, enabling:

- Fine adjustment of the LO drive level,
- Compensation of frequency-dependent losses,
- Optimization of mixer conversion efficiency and linearity.

Stable LO power is essential to guarantee consistent conversion gain and to avoid performance degradation in both Tx up-conversion and Rx down-conversion paths.

Spectral Purity and Phase Noise

High spectral purity is a fundamental requirement for THz heterodyne systems. The LO chain incorporates:

- A low-phase-noise PLL synthesizer (based on a fractional-N architecture),
- Frequency multiplication stages (×4) to reach the required LO band,
- A tunable bandpass filter to suppress unwanted harmonics and spurious components.

This architecture ensures:

- Low phase noise, minimizing reciprocal mixing and preserving receiver sensitivity,
- Suppression of spurious tones, which is essential for high-order modulation schemes and wideband communication,
- Stable frequency generation across the entire tuning range.

Phase noise performance is particularly critical at THz frequencies due to multiplication effects, where phase noise degrades proportionally to the multiplication factor.

Reference Clock and Frequency Stability

The LO subsystem relies on a shared high-stability reference clock generated by a 100 MHz voltage-controlled crystal oscillator (VCXO).

Key characteristics include:

- Distribution of a common reference to both Tx and Rx PLLs,
- Filtering of reference harmonics to ensure clean locking conditions,
- Support for coherent system operation, which is essential for:
    - Stable frequency translation,
    - Phase alignment between Tx and Rx paths,
    - Advanced functionalities such as beamforming and coherent detection.

The use of a common reference guarantees deterministic frequency relationships across the system and reduces long-term frequency drift.

Control Interface and Agility

The LO subsystem is fully integrated into the digital control architecture of the front-end. Configuration and monitoring are achieved via:

- SPI communication interface for PLL programming,
- Microcontroller-based control unit handling initialization and frequency management,
- Hardware stepping interface for rapid frequency switching without software overhead.

This enables:

- Fast retuning capability, suitable for dynamic scenarios,

- Automated calibration and monitoring, improving system robustness,
- Repeatable configuration, with parameters stored in non-volatile memory.

Such flexibility is essential for both laboratory characterization and field deployment scenarios.
Integration and Interface Considerations
The LO signals are delivered to the RF modules through high-frequency coaxial interfaces (1.85 mm connectors), ensuring:

- Low insertion loss,
- High repeatability,
- Compatibility with the targeted frequency range.

Careful routing and shielding are implemented to:

- Minimize electromagnetic interference (EMI),
- Prevent coupling between LO, RF, and digital signals,
- Preserve signal integrity in a compact integrated environment.

The LO subsystem fulfills all requirements for high-performance THz heterodyne front-ends, combining frequency agility, spectral purity, and robust digital control. Its architecture—based on PLL synthesis, frequency multiplication, and integrated filtering—provides a scalable and reliable solution for both Tx and Rx operation, enabling stable and efficient frequency conversion across the targeted THz band.

Electrical specifications of the LO	Achieved	Predefined
LO_1 (first LO)output frequency PLL-VCO (GHz)	24-33.6	25 … 35
LO multiplication factor on the BE (unfiltered x N_{BE})	N_{BE} = 4	N_{BE} = 4
LO multiplication factor on the FE (unfiltered x N_{FE})	N_{FE} = 8	N_{FE} = 4
LO output frequency at up/downconverter MMIC (GHz) $F_{LO}=(N_{FE}*F_{LO1})$	192-268.8	80 – 120
LO switching speed	N/A	TBD
Output Power	3-7 dBm	TBD
Frequency Tuning	Discrete steps (digital control)	TBD

Tab. 10: General specifications of the local oscillator (LO_1) that is to be coupled to the up/down converters.

4.1.4 Indoor Units

The Indoor Unit (IDU) represents the central integration platform of the TIMES THz front-end system, combining all RF, LO generation, control, and power subsystems into a compact and deployable module. It is designed to provide a fully functional heterodyne transceiver solution operating in the 275–325 GHz frequency range, with intermediate frequency (IF) interfaces in the 60–90 GHz band.

System Architecture

The IDU integrates the complete transmit and receive chains, including:

- Tx and Rx waveguide front-end modules,
- Medium Power Amplifier (MPA),
- Dual PLL-based LO generation units,
- Embedded control and monitoring electronics.

The architecture supports full-duplex operation, with independent LO paths for Tx and Rx, enabling simultaneous transmission and reception. RF interfaces are realized via WR-3.4 waveguide ports, while IF signals are handled through WR-12 interfaces, ensuring low-loss signal routing across all frequency domains. In the transmit path, the IF signal (60–90 GHz) is upconverted to the THz band using the LO signal and subsequently amplified by the MPA before being delivered to the RF output. In the receive path, incoming THz signals are first amplified and then downconverted to the IF band using a dedicated LO chain.

Mechanical Integration and Packaging

The IDU is implemented within a compact metallic enclosure with dimensions of approximately 17.2 × 8.9 × 7.2 cm^3, designed to ensure mechanical robustness, electromagnetic shielding, and efficient thermal management.

The internal structure follows a layered architecture:

- The upper layer hosts the RF modules (Tx, Rx, MPA),
- The lower layers contain the PLL boards and DC power management circuitry,
- Interconnections between layers are realized using high-frequency coaxial cables optimized for minimal loss and controlled bending radius.

The use of CNC-milled, gold-plated waveguide housings ensures:

- Low conductor losses at THz frequencies,
- Stable RF grounding,
- High repeatability and mechanical precision.

Short waveguide interconnects are employed between modules to minimize insertion loss and preserve signal integrity.

RF Performance and Signal Integrity

The IDU architecture is optimized for broadband operation across the targeted THz band. Key design considerations include:

- Minimization of waveguide losses through short interconnect paths,
- Efficient MMIC-to-waveguide transitions using E-plane probe structures,
- Isolation between Tx and Rx paths to prevent self-interference.

The integration of the MPA directly within the RF chain ensures sufficient output power while maintaining spectral purity. The modular design allows operation both with and without the MPA, facilitating flexible testing and deployment configurations.

Control and Digital Interface

A central feature of the IDU is the embedded microcontroller-based communication controller, which manages all system-level functions, including:

- Initialization and bias sequencing,
- PLL configuration and frequency control,
- Telemetry acquisition and system monitoring,
- Digital communication with external systems.

The controller communicates with the PLLs and RF subsystems via SPI interfaces, while USB connectivity provides a user interface for configuration and data exchange.

This digital infrastructure enables:

- Automated system tuning,
- Real-time monitoring of operating conditions,

- Simplified integration into higher-level communication systems.

Power Supply and Thermal Management

The IDU is powered via a centralized DC input stage, which distributes regulated voltages to all subsystems. The power architecture includes:

- Local voltage regulation for RF and digital components,
- Bias generation for MMIC operation,
- Monitoring of current consumption and system health.

Thermal management is achieved through:

- The metallic enclosure acting as a heat spreader,
- Vertical stacking of components to separate heat-generating elements,
- Efficient conduction paths from MMICs to the housing.

This approach ensures stable operation under continuous high-frequency operation without the need for complex active cooling solutions.

Modularity and Scalability

The IDU is designed with a strong emphasis on modularity, allowing:

- Independent development and replacement of Tx, Rx, and LO subsystems,
- Rapid reconfiguration for different experimental setups,
- Scalability toward future system upgrades.

The separation of RF, LO, and control domains facilitates:

- Improved isolation,
- Simplified debugging and testing,
- Flexibility in adapting to different use cases and frequency plans.

The Indoor Unit constitutes a fully integrated, compact, and high-performance THz transceiver platform, combining advanced RF design, precise LO generation, and robust digital control. Its architecture demonstrates the feasibility of scalable and deployable THz communication systems, providing a solid foundation for both laboratory validation and future real-world applications.

Fig. 4: Indoor unit incorporating the THz Rx and Tx modules as well as the LO generation and the required periphery and interfaces..

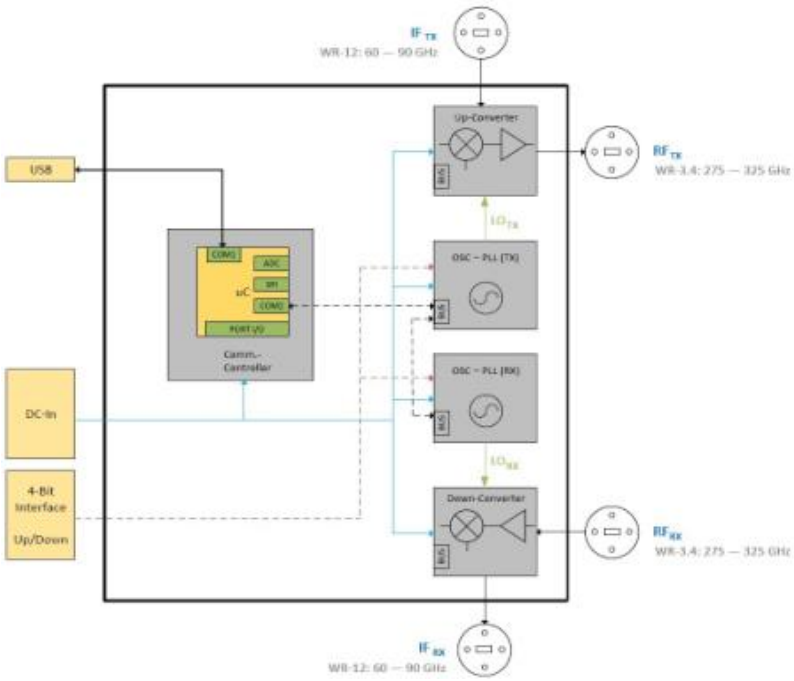

Fig. 5: Simplified block diagram of the indoor unit.

Interface specifications RX/TX IU	Achieved	Predefined
RF frequency range (GHz)	275 – 325 GHz	280…320
RF output power (dBm, OP1dB)	8	5
TX conversion gain (dB)	30	30

IF frequency range (GHz)	60-90	60…>90
IF input power (dBm, IP1dB)	-25	-15
Rx conversion gain (dB)	12	12
Rx P1dB (dBm)	-30	TBD
Operation mode	Full Duplex	Full Duplex
RF interfrace	WR-3.4 waveguide	WR-3.4 waveguide
IF interfaces	WR-12 waveguide	WR-12 waveguide
Dimensions	17.2 × 8.9 × 7.2 cm³	TBD
Control interface	SPI / USB via microcontroller	SPI / USB via microcontroller
Power supply	Central DC input with local regulation	Central DC input with local regulation

Tab. 11: General specifications of the IU modules.

4.1.5 Front-End requirements for the implementation of the different

Within the project two PoCs are defined, which are: PoC1 with FDD-modems and high-gain antennas and PoC 2 utilizing the beam-steerable antennas. And TDD-modems. Each PoC brings its own demands in system architecture:

PoC 1 – FDD-Concept using high-gain antennas: In this scenario, due to the larger antenna dimensions, a single antenna should be used for both the R_X and T_X path at each node. This antenna has to handle the transmitted and received signals. As indicated in the earlier deliverable D2.3, "only a diplexer can provide the required isolation above 50 dB between the R_X and T_X path. The isolation of other components such as couplers is typically limited to the same range as the return loss, which is typically in the range of 25 dB and much too low for the targeted application."

The diplexer is, as initially planned, realized as a separate waveguide component to connect the R_X and T_X path/modules (see Fig. 9, the initial plan and Fig. 10 the project result with measured s-Parameters). The design procedure had been published in [10].

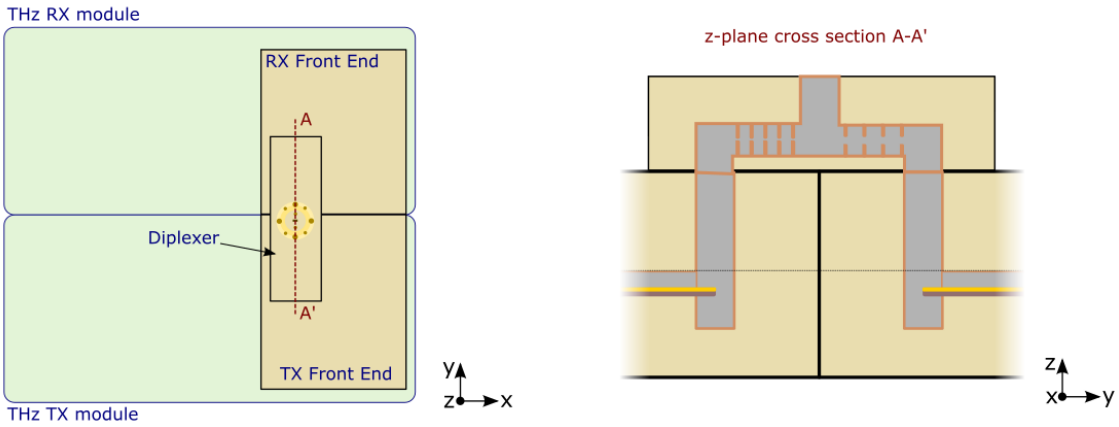

Fig. 6 Preliminary schematic view of the waveguide diplexing structures to combine two separated FEs (Rx and Tx) in a single waveguide fed (WR3.4) antenna.

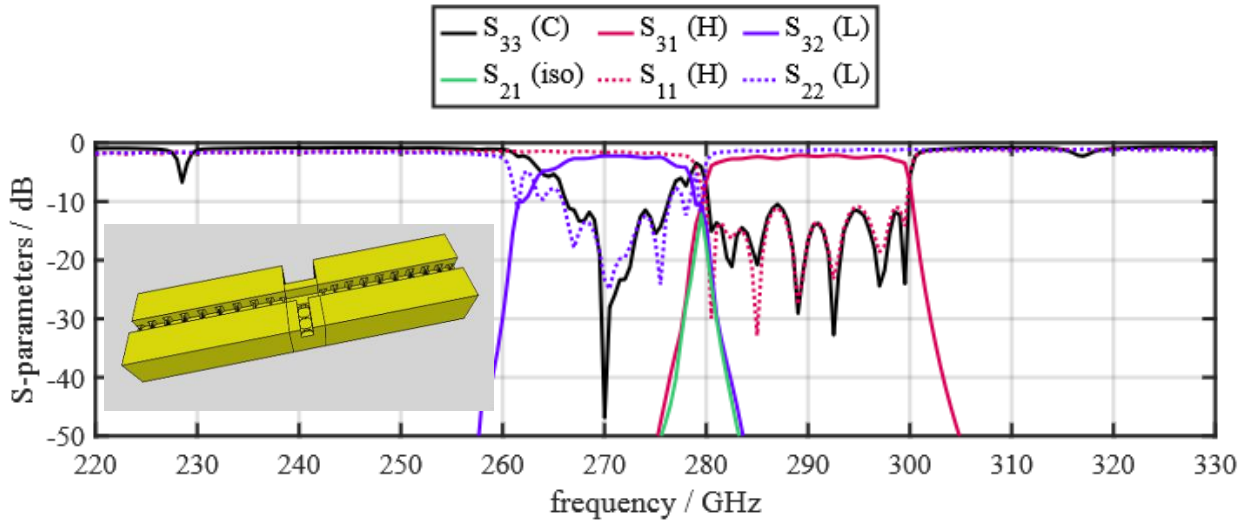

Figure 7: Final measurements of the designed diplexer for PoC1 with a rendering of the step file as inlay.

Scenario 2 – Using beam-steerable antennas and TDD-modems:

In the beginning of the project, this scenario was planned using a separate antenna for each, RX and TX "since both must be able to use the whole and same frequency range provided by the antenna." During the project, it showed, that the manufacturing of the antennas is difficult, so that only a limited number of antennas could be produces. Also, the antennas are, in spite of the small wavelength of the signals, spatially bulky which prevents a mounting close to each other. For these reasons, within the project, broadband waveguide couplers are employed to connect RX and TX to a common antenna port. As illustrated in the previous section, waveguide coupler yield lower isolation between the ports, but as TDD-modems are used, the limited isolation is found to be of limited impact.

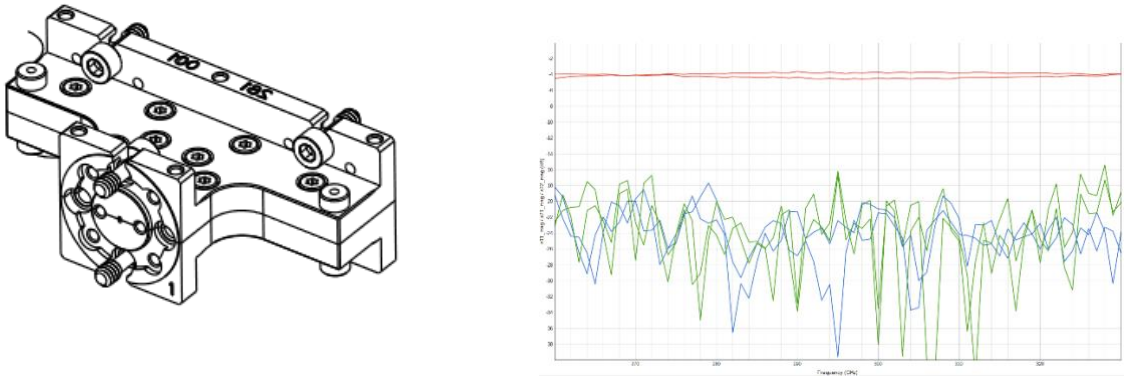

Figure 8: Employed combiner for PoC2 with mechanical drawing and measured S-parameters.

4.2 Overall outcome of the PoC1 - AETNA

POC1-AETNA have been conducted on 16/3/26 to 20/03/2026 in AETNA Techlab that represent an Industrial Envinronment. The two radio station are at 90° and in NLOS, the total distance is 38,6m and the beam reflection is achieved by a passive RIS with 30° of orientation angle.

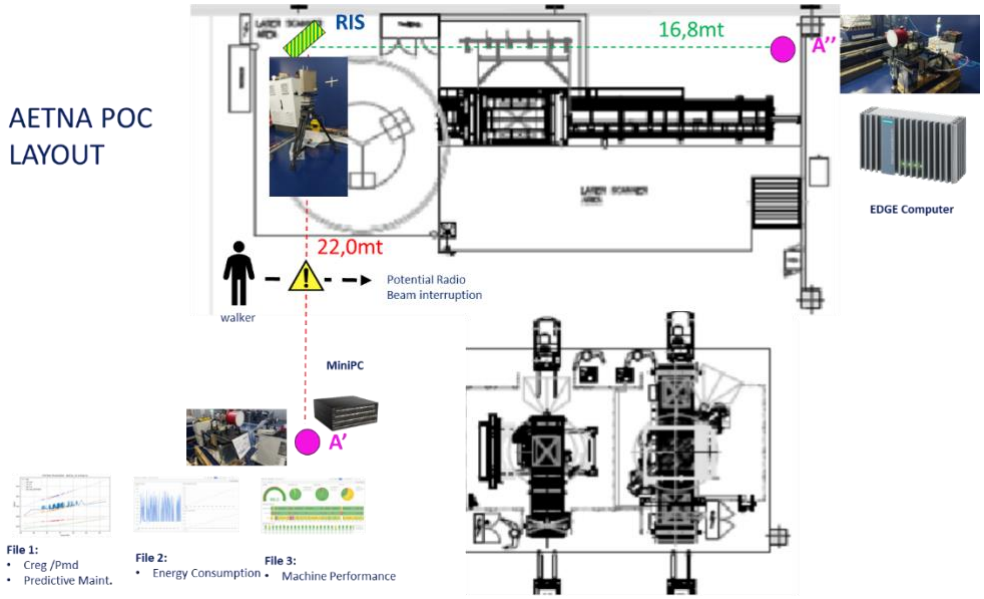

Figure 9: AETNA-POC1 Layout in Techlab.

The Transmitting Device is an Industrial EDGE Computer and the receiving Device is a Mini PC.

In the Industrial Edge Computer are collect 10Gbyte of data collected in one year of data acquisition of real machine in production

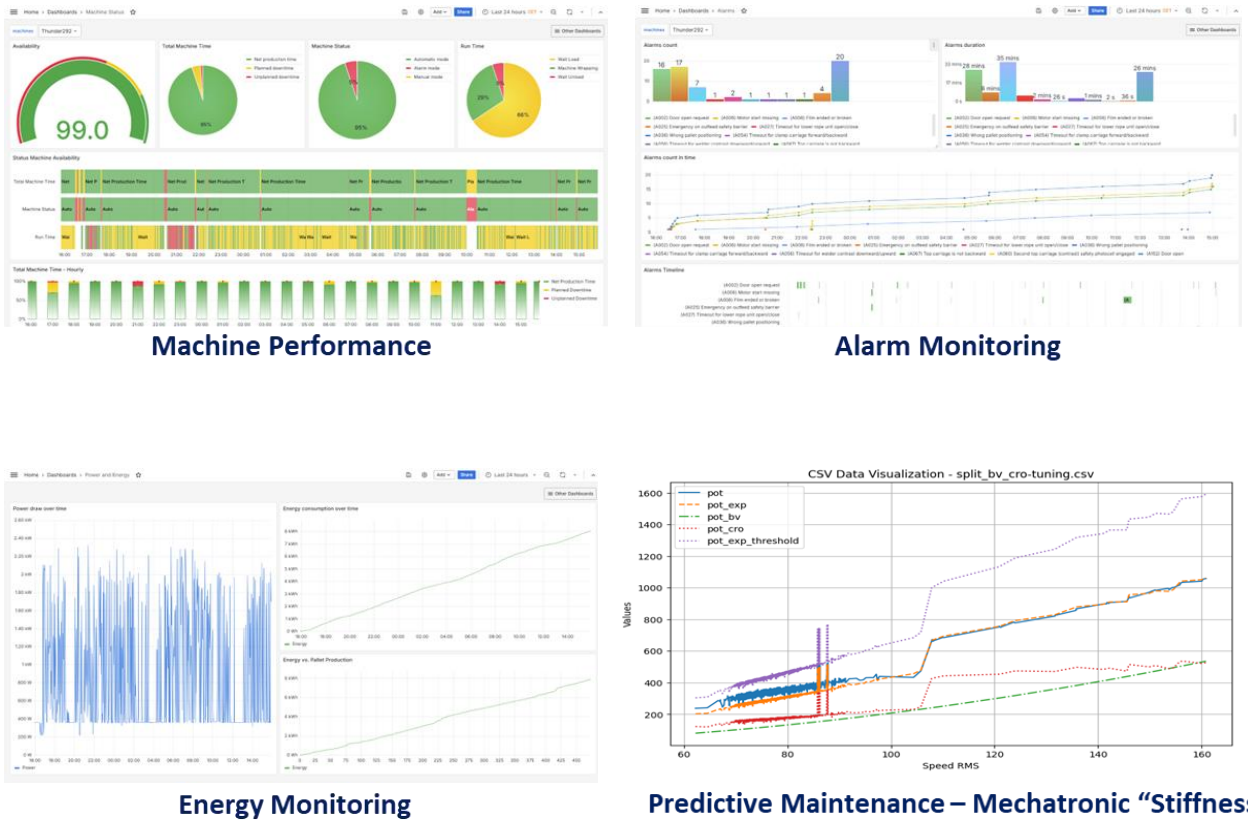

Figure 10: Main Data Dashboard pf Transmitted Data.

The entire DB of 10Gb have transmitted continuously for 1260 time, for a total data exchange of 12.6TBytes. No data have been lost, the average data rate was 0.94Gbit/s, this limitation is due to a limit in the ethernet port of Edge Computer and mini PC (1Gbps)

In following table we compare different types of communication connections, the first four rows are related to a standard connection (wired and WiFi), the last two rows in magenta are related to the connection with THZ device in POC1- AETNA. It is interesting to observe that the "Delay Jitter" decreases with respect to the standard connection

Condition	Speed (Mbit/s)	Delay Jitter	Notes
Ethernet (1 Gbit/s) Wired	940	0,032 ms	Near theoretical max
WiFi (2.4GHz, close)	100	0,151 ms	
WiFi (2.4GHz, PoC dist.)	70	0,536 ms	Signal degradation through wall

WiFi (5GHz, close)	150	ND	Unstable and limited to 20 MHz channel due to noisy environment
TeraHz (Metal Plate)	941	0,012 ms	Limited to 1Gbit/s by the network equipment
TeraHz (RIS)	941	0,008 ms	Limited to 1Gbit/s by the network equipment

Tab. 12: Speed and Jitter value in different Transmission Test (in agenta POC1 condition).

References

[9] L. Gebert et al., "A Superheterodyne 300 GHz InGaAs Receiver and Transmitter Chipset for 6G and Beyond Applications," 2025 20th European Microwave Integrated Circuits Conference (EuMIC), Utrecht, Netherlands, 2025, pp. 41-44, doi: 10.23919/EuMIC65284.2025.11234400.

[10] S. Haussmann et al., "H-Band Waveguide Filters for Duplex THz Communications," *2025 16th German Microwave Conference (GeMiC)*, Dresden, Germany, 2025, pp. 350-353, doi: 10.23919/GeMiC64734.2025.10979193